Long-term restoration of visual function in end-stage retinal degeneration using subretinal human melanopsin gene therapy

Samantha R. De Silva[a], Alun R. Barnard[a], Steven Hughes[a], Shu K. E. Tam[a], Chris Martin[b], Mandeep S. Singh[a], Alona O. Barnea-Cramer[a], Michelle E. McClements[a], Matthew J. During[c], Stuart N. Peirson[a], Mark W. Hankins[a,1], and Robert E. MacLaren[a,d,1]

[a]Nuffield Laboratory of Ophthalmology, Nuffield Department of Clinical Neurosciences, University of Oxford, National Institute for Health Research Biomedical Research Centre, Oxford OX3 9DU, United Kingdom; [b]Department of Psychology, The University of Sheffield, Sheffield S1 2LT, United Kingdom; [c]The Ohio State University, Columbus, OH 43210; and [d]Moorfields Eye Hospital, National Institute for Health Research Biomedical Research Centre, London EC1V 2PD, United Kingdom

Edited by King-Wai Yau, Johns Hopkins University School of Medicine, Baltimore, MD, and approved August 29, 2017 (received for review January 30, 2017)

Optogenetic strategies to restore vision in patients who are blind from end-stage retinal degenerations aim to render remaining retinal cells light sensitive once photoreceptors are lost. Here, we assessed long-term functional outcomes following subretinal delivery of the human melanopsin gene (OPN4) in the *rd1* mouse model of retinal degeneration using an adeno-associated viral vector. Ectopic expression of OPN4 using a ubiquitous promoter resulted in cellular depolarization and ganglion cell action potential firing. Restoration of the pupil light reflex, behavioral light avoidance, and the ability to perform a task requiring basic image recognition were restored up to 13 mo following injection. These data suggest that melanopsin gene therapy via a subretinal route may be a viable and stable therapeutic option for the treatment of end-stage retinal degeneration in humans.

human melanopsin | gene therapy | optogenetics

Inherited retinal degenerations such as retinitis pigmentosa (RP) affect 1 in 4,000 people (1), causing significant visual morbidity and blindness due to a progressive loss of photoreceptor cells. Even in end-stage disease, the remaining retinal layers and central visual projections remain structurally intact. Stimulation of these remaining cells is potentially sufficient to mimic visual responses and restore vision, and by this means the subretinal electronic implant has shown proof of principle for restoration of vision in patients after severe photoreceptor loss (2).

An alternative gene therapy strategy involves the expression of transgenes encoding photosensitive proteins in remaining retinal cells, making them directly light sensitive in the absence of rods and cones (3–7). A candidate protein for this purpose is melanopsin, the photopigment naturally present in a subset of ganglion cells that are intrinsically photosensitive [intrinsically photosensitive retinal ganglion cells (ipRGCs)] (8). Melanopsin is particularly suited to this purpose since it is native to the human eye (9) and therefore is less likely to be immunogenic. Melanopsin shows greater sensitivity to light than alternative microbial optogenetic tools such as channelrhodopsin-2 (3, 10, 11) or halorhodopsin (4), but has slower kinetics. Furthermore, the melanopsin transduction cascade involves the activation of ubiquitously expressed Gnaq/11-type G proteins (12), permitting signal amplification in multiple host cell types (13, 14).

Previous work used intravitreal delivery of an adeno-associated viral (AAV) vector to express mouse melanopsin in ganglion cells with restoration of visual responses (5). We investigated whether human melanopsin (OPN4) could be effectively delivered via an alternative subretinal approach, using a ubiquitous (CBA) promoter to drive expression in all remaining outer retinal cells for several reasons. Subretinal vector delivery is well established in human clinical trials (15, 16) but has not been assessed in combination with a CBA promoter as an optogenetic approach for vision restoration. Transduction of cells in the upstream retina maximizes the potential of retaining complex processing of the visual signal. Furthermore, increased availability of chromophore (retinal) in the outer retina may be required for effective photon capture in the absence of specialized outer segment discs. Other studies have used AAV vectors containing a mouse bipolar-cell–specific enhancer to target a melanopsin.mGluR6 chimera (17) or rhodopsin (6) to bipolar cells via intravitreal injection. However, there is variation in anatomy between primates and mouse models (18), and this may render the intravitreal approach less effective in humans. Virions delivered via intravitreal injection are diluted more in primates compared with mice due to the larger volume of the vitreous, reducing the concentration of vector reaching retinal cells. The inner limiting membrane on the retinal surface is also thicker in primates than in rodents (19), through which virions must pass to reach target cells. The increased risks of an inflammatory response following intravitreal AAV injection (20) may also limit the translational potential of this route of delivery. We therefore assessed

Significance

Inherited retinal degenerations may result in blindness due to a progressive loss of photoreceptor cells. We assess subretinal delivery of human melanopsin using an adeno-associated viral vector to remaining retinal cells in a model of end-stage retinal degeneration. Human melanopsin, being already present in the eye, is unlikely to generate an immune response when introduced via gene therapy. Furthermore, this method of delivery has been proven to be safe in clinical trials and may be more effective at delivering vector in primates than the alternative method of intravitreal injection. We demonstrate long-term vector expression and restoration of visual function, indicating that this therapy could be stable and efficacious in the treatment of patients with end-stage retinal degenerations.

Author contributions: S.R.D.S., A.R.B., S.H., S.K.E.T., M.E.M., M.W.H., and R.E.M. designed research; S.R.D.S., A.R.B., S.H., S.K.E.T., C.M., M.S.S., and A.O.B.-C. performed research; S.K.E.T., C.M., M.E.M., M.J.D., and S.N.P. contributed new reagents/analytic tools; S.R.D.S., S.H., and C.M. analyzed data; and S.R.D.S., A.R.B., M.W.H., and R.E.M. wrote the paper.

Conflict of interest statement: S.R.D.S., A.R.B., M.W.H., and R.E.M. are listed as inventors on a patent submitted by the University of Oxford relevant to this work. R.E.M. is a founding director of Nightstarx Ltd., a retinal gene therapy company established by the University of Oxford and owned by the Wellcome Trust. M.W.H. is listed as an inventor on a patent owned by Imperial College London relating to restoring light responses by ectopic expression of melanopsin.

This article is a PNAS Direct Submission.

Freely available online through the PNAS open access option.

[1]To whom correspondence may be addressed. Email: mark.hankins@eye.ox.ac.uk or enquiries@eye.ox.ac.uk.

This article contains supporting information online at www.pnas.org/lookup/suppl/doi:10.1073/pnas.1701589114/-/DCSupplemental.

transduction following subretinal delivery of OPN4 and whether this could support long-term restoration of light sensitivity and visual function in a mouse model of end-stage RP.

Results

Long-Term Expression of Human Melanopsin in Degenerate Retina Is Achieved Following Subretinal Delivery of an AAV Vector. To model the extensive photoreceptor loss seen in end-stage RP, the *rd1* mouse was used. These mice have a nonsense mutation in the *Pde6b* gene, which leads to rapid degeneration of rod photoreceptors followed by loss of cones (21). Retinal tropism was assessed 4 and 15 mo after subretinal delivery of a single capsid mutant AAV vector [rAAV2/8(Y733F) CBA-*OPN4*-IRES-DsRed] in 6- to 8-wk-old *rd1* mice. This bicistronic vector included a DsRed fluorescent marker to permit visualization of transduced cells within the retina and ensure vector-driven expression. Retinal flatmounts stained with human OPN4-specific antibody showed widespread retinal transduction in treated eyes, which was sustained up to 15 mo postinjection (Fig. 1 *A* and *B*), but none in age-matched untreated controls (Fig. 1 *C* and *D*). Human melanopsin showed appropriate membrane localization (Figs. S1 and S2*E*), with the DsRed marker confirming vector-driven expression (Fig. 1*E*). Histological sections demonstrated robust and widespread OPN4 expression throughout the inner nuclear and inner plexiform layers of the degenerate retina in treated eyes, with immunohistochemistry using horizontal, bipolar (Fig. 1 *F* and *G*, and Fig. S1), and Müller cell (Fig. S2)-specific antibodies and cell morphology indicating widespread transduction of these cell types. There was no significant transduction of cell bodies in the ganglion cell layer following subretinal vector delivery, as assessed by cell morphology and ganglion cell-specific staining (Fig. S2).

Human Melanopsin Expressed in the Degenerate Retina Is Able to Mediate a Functional Response to a Light Stimulus. Expression of the "immediate early" gene c-Fos is a marker of cellular depolarization and has been widely used to monitor melanopsin-driven light responses in ipRGCs in the degenerate retina (22, 23). Comparison of light-induced c-Fos expression in the inner nuclear layer (INL) of vector-treated versus untreated retina showed a 2.5-fold increase in the number of c-Fos–positive cells in treated eyes (effect of treatment, $P = 0.0197$, two-way ANOVA; Fig. S3 *A–G*). High levels of colocalization were observed for both DsRed and c-Fos (Fig. S3 *A–C*), and human OPN4 and c-Fos (Fig. S3 *O–Q*), confirming light-induced depolarization of transduced cells in treated retina. In addition, some adjacent c-Fos–positive cells were observed that did not appear to express OPN4 (or DsRed), which might indicate depolarization of neighboring cells and cell-to-cell signaling resulting from ectopic expression of OPN4 in the degenerate retina.

Multielectrode array (MEA) recordings from ex vivo retinal explants were performed 4 mo after subretinal vector delivery to assess whether expression of OPN4 in the INL was able to drive action potential firing in retinal ganglion cells, and therefore generate a signal that could be centrally transmitted. The percentage of electrodes showing a light-dependent increase in action potential firing in treated retinas (43.1 ± 5.6% electrodes, $n = 6$ retinas, $n = 144$ electrodes) was more than doubled compared with untreated age-matched controls (18.1 ± 7.3% electrodes, $n = 9$ retinas, $n = 88$ electrodes; $P = 0.028$, two-tailed unpaired t test; Fig. 2*A*). Responses observed in untreated retina were consistent with the activation of endogenous ipRGCs, whereas treated retinas include both these responses and those originating from ectopic expression of human OPN4 (Fig. 2*C*). In treated but not untreated retina, some electrodes showed a reduction in spike firing rate following light stimulation (Fig. 2*B*), which may add to the complexity of the visual signal generated following OPN4 expression in inner nuclear cells. Visualization of DsRed fluorescence using 540-nm light (Fig. 2*D*) confirmed that the location of responsive electrodes in treated retinas was highly correlated to areas transduced by the OPN4 vector (Fig. 2 *C–E* and Fig. S4*A*), indicative of these being responses from ectopically expressed OPN4.

Irradiance response curves (IRCs) generated for responsive electrodes in retinas following vector delivery ($n = 51$ electrodes,

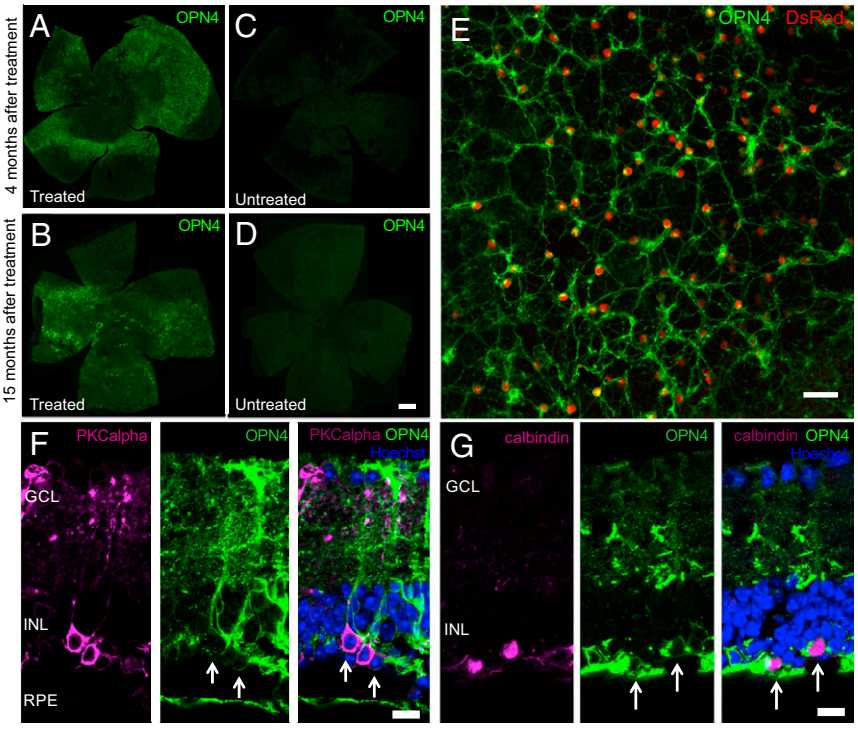

Fig. 1. Long-term expression of human melanopsin is achieved in the degenerate retina following subretinal delivery of an adeno-associated viral (AAV) vector. Flatmounts of the *rd1* mouse retina assessed following immunolabeling for human OPN4 (green) at 4 mo (*A*) and 15 mo (*B*) after subretinal OPN4 vector delivery reveal widespread transduction. Labeling of human OPN4 was absent from untreated age-matched controls (*C* and *D*). (Scale bar, 500 μm.) Images *A–D* are composite fluorescence images each of a single mouse retina. Appropriate membrane localization of human melanopsin was evident demonstrating a network of transduced cells, with DsRed fluorescence confirming vector-driven OPN4 expression (*E*). (Scale bar, 25 μm.) Successful transduction of bipolar cells (labeled by PKCα, purple, *F*) and horizontal cells (labeled by calbindin, purple, *G*) using a ubiquitous promoter was evident following colabeling with OPN4 (green) and Hoechst nuclear stain (blue). (Scale bar, 25 μm.)

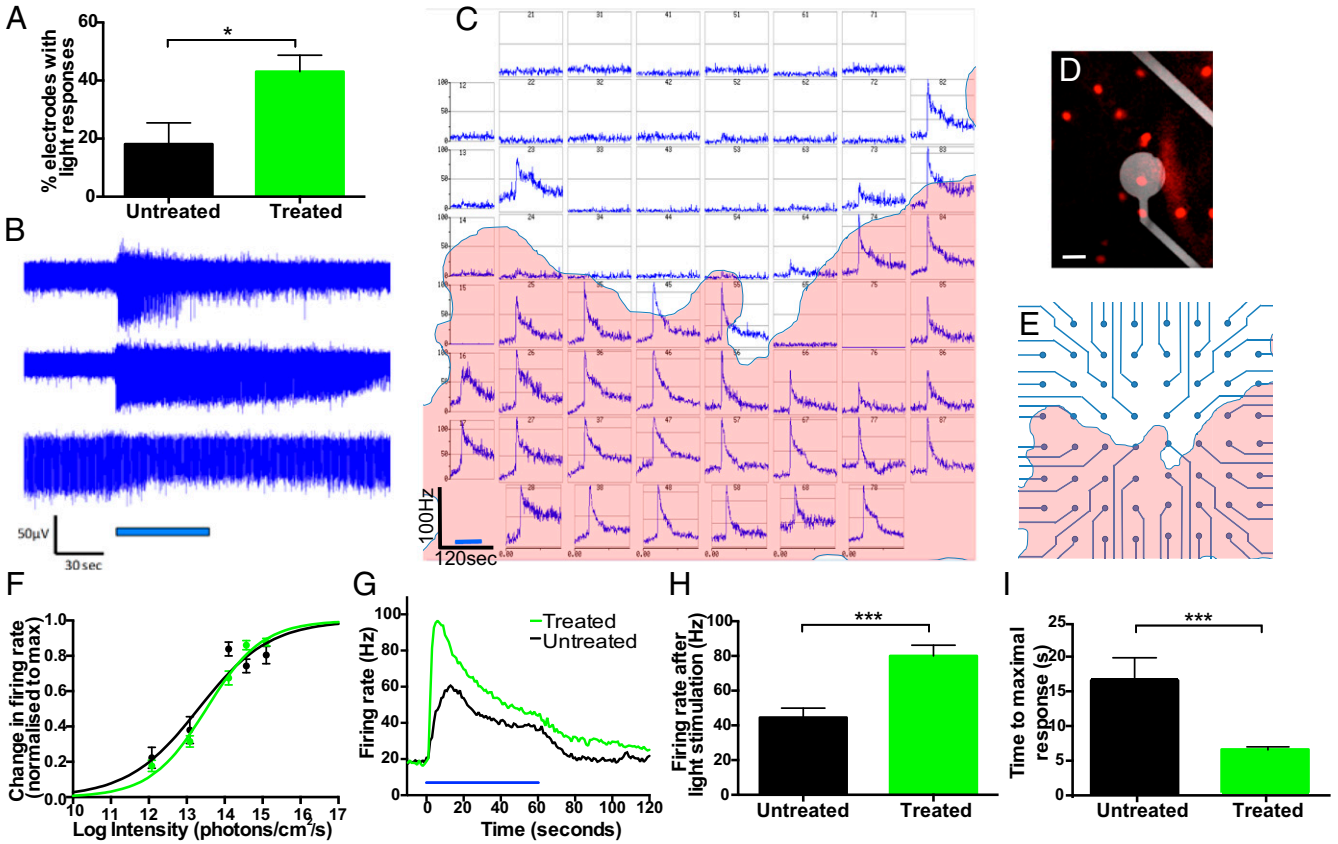

Fig. 2. Human melanopsin expressed in the degenerate retina is able to mediate a functional response to a light stimulus. Multielectrode array (MEA) recordings from ex vivo *rd1* mouse retinas showed a higher percentage of electrodes demonstrating light-induced increases in action potential firing in treated retinas compared with untreated controls (*A*) ($P = 0.028$, two-tailed unpaired *t* test; treated, $n = 6$; untreated, $n = 9$). Examples of raw data obtained from individual electrodes following 60-s 480-nm light pulses are shown (*B*). Light responses recorded from electrodes from one treated retina are shown (*C*) [represented as mean spike firing rate (in hertz) measured in 1-s bins; data shown are 30 s of baseline recording followed by a 60-s 480-nm light stimulus at 3.99×10^{14} photons·cm^{-2}·s^{-1}; for original image of the retina showing location of DsRed-positive cells, see Fig. S4]. Visualization of DsRed fluorescence (dots) illustrates the area of the retina transduced by the human OPN4 vector relative to the position of MEA recording electrodes (*D*). (Scale bar, 15 μm.) A representation of DsRed expression (highlighted in red) is shown to indicate the transduced areas of the treated retina in *C* relative to the positioning of electrodes (*E*). In combination, this illustrates an increase in light-dependent action potential firing within regions of transduced retina. IRCs generated from responsive electrodes in treated ($n = 51$ electrodes, $n = 3$ retinas) and untreated ($n = 22$ electrodes, $n = 4$ retinas) retinas show a similar sensitivity of responses between groups (*F*), with action potential firing detected at the lowest light intensity assessed (1.20×10^{12} photons·cm^{-2}·s^{-1}). The mean response of all electrodes to a 3.99×10^{14} photons·cm^{-2}·s^{-1} light stimulus is shown (*G*). Blue bars indicate duration of light stimuli (*B*, *C*, and *G*). There was a greater increase in spike firing rate in response to a light stimulus in treated versus untreated retinas (*H*); and time to maximal response was shorter in treated retinas compared with untreated controls (*I*) (***$P < 0.001$, two-tailed unpaired *t* test). For further description of response kinetics, see Fig. S4.

$n = 3$ retinas) versus controls ($n = 22$ electrodes, $n = 4$ retinas) revealed similar overall light sensitivity between groups (Fig. 2*F*): with half-maximal responses (EC_{50}) observed at 13.4 ± 0.11 log photons·cm^{-2}·s^{-1} in electrodes from treated retina versus 13.2 ± 0.16 in controls ($P = 0.26$, two-tailed unpaired *t* test). However, at subsaturating levels of light (3.99×10^{14} photons·cm^{-2}·s^{-1}), the maximal spike firing rate was significantly higher on responsive electrodes from treated retinas (80.0 ± 6.2 Hz, $n = 54$) versus untreated controls (44.6 ± 5.4 Hz; $n = 25$; $P = 0.0006$, two-tailed unpaired *t* test; Fig. 2 *G* and *H*). A range of response kinetics was observed for both treated and untreated groups, including transient and sustained changes in action potential firing (Fig. 2*B* and Fig. S4 *B* and *C*). At subsaturating levels of light (3.99×10^{14} photons·cm^{-2}·s^{-1}), the time taken to reach maximal firing rate was significantly lower on electrodes from OPN4-treated retinas (6.63 ± 0.5 s; $n = 54$) compared with untreated controls (16.9 ± 2.9 s; $n = 25$; $P < 0.0001$, unpaired *t* test; Fig. 2*I*), indicating different response kinetics between ganglion cells firing in OPN4-treated retinas versus responses recorded from native ipRGCs in untreated controls.

Visual Function Restored by Human Melanopsin Expression in the Degenerate Retina Was Sustained at 13 mo. The pupil light reflex (PLR) was evaluated to determine whether light-dependent signals generated by ectopic OPN4 expression could affect central targets. Mice that received a unilateral subretinal injection of OPN4 vector were compared with age-matched mice that received a sham injection of PBS and also with untreated controls. The consensual PLR was assessed to avoid any surgical effect on pupil constriction in the treated eye. Two cohorts of mice were evaluated, one at 2 mo after injection (Fig. S5) and another at 13 mo to determine long-term functional improvement. Thirteen months after OPN4 vector delivery, pupil constriction was significantly greater in treated eyes compared with controls at multiple light intensities (overall treatment effect, $P = 0.013$, repeated-measures two-way ANOVA; Fig. 3 *A* and *B*). Pupil constriction was faster in the OPN4 vector group compared with sham-injected and untreated groups (interaction between treatment and time on pupil area: $P < 0.0001$, repeated-measures two-way ANOVA; Fig. 3*C*). Furthermore, pupil constriction was significantly reduced in older sham-injected (effect of age, $P = 0.0018$, repeated-measures two-way ANOVA) and untreated ($P = 0.0067$) control groups

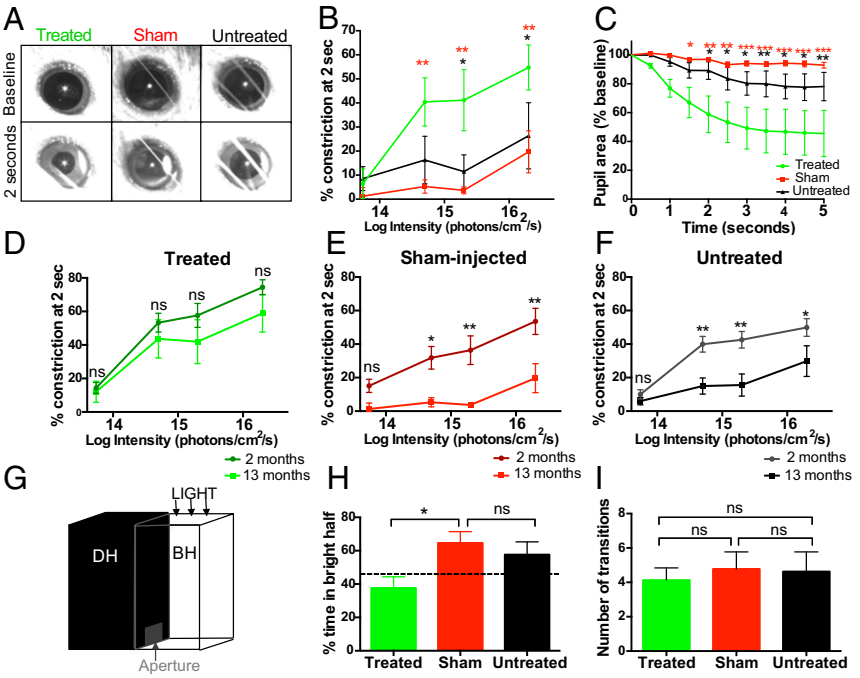

Fig. 3. Visual function restored by human melanopsin expression in the degenerate retina was sustained at 13 mo. Representative images show levels of pupil constriction observed 13 mo after human OPN4 vector delivery, compared with age-matched sham-injected and untreated controls (*A*). Significantly more pupil constriction was observed in mice treated with OPN4 vector compared with sham-injected (red*) and untreated controls (black*), at multiple light intensities (*B*) measured at 2 s after light onset (treated, $n = 5$; sham-injected, $n = 8$; untreated, $n = 13$). Time course of pupil constriction at 2×10^{15} photons·cm^{-2}·s^{-1} demonstrated a faster response in the treated group (*C*). Pupil constriction was not significantly different in treated mice (*D*) at 2 and 13 mo, whereas the level of pupil constriction declined with age in sham-injected (*E*) and untreated mice (*F*) (2-mo cohort: treated, $n = 10$; sham-injected, $n = 9$; untreated, $n = 12$; ns, nonsignificant; $*P < 0.05$, $**P < 0.01$, repeated-measures two-way ANOVA with Tukey post hoc test). In the behavioral light–dark assay, mice could move freely between the bright half (BH) of the test chamber illuminated by a white light stimulus of 200 lx at ground level and the dark half (DH) (*G*). Mice treated with OPN4 vector 13 mo previously spent less time in the bright half of the chamber compared with sham-injected controls (*H*) (treated, $n = 8$; sham-injected, $n = 9$; untreated, $n = 8$; $P = 0.03$, one-way ANOVA with Tukey post hoc test). The number of transitions between compartments was similar across groups (*I*).

compared with their younger counterparts (Fig. 3 *E* and *F*). This effect was not seen in the OPN4 vector-treated group ($P = 0.217$; Fig. 3*D*), indicating a sustained treatment effect in the older cohort following OPN4 vector delivery.

To assess whether information generated by ectopic expression of OPN4 in the retina could drive visually guided behavior, animals were assessed using a behavioral light avoidance assay (24, 25) based on the natural preference of mice to avoid brightly lit environments (Fig. 3*G*). Thirteen months after OPN4 vector delivery, there was a significant difference in the percentage of time spent in the brightly lit chamber between groups (treated, 37.65% ± 6.7; sham-injected, 64.66% ± 6.8; untreated, 57.65% ± 7.7; $P = 0.03$, one-way ANOVA; Fig. 3*H*), with the vector-treated group showing behavior closest to wild-type mice. This was not due to a difference in general or anxiety-related locomotor activity, since the number of transitions between light and dark chambers was similar between groups ($P = 0.88$, one-way ANOVA; Fig. 3*I*). Functional effects seen were unlikely to be mediated by residual cones in the *rd1* mouse, since these cells were morphologically abnormal and there was no difference in numbers of remaining cells between treated, sham-injected, and untreated groups (Fig. S6 *A–D*; $P = 0.123$, one-way ANOVA). Furthermore, all *rd1* mice selected were homozygous for the *gpr179* mutation (Fig. S6 *E* and *F*), excluding any input from residual photoreceptors in mediating ON bipolar cell depolarization via the mGlur6 cascade in this mouse model (26).

Visual Responses Requiring Image-Forming Vision Are Generated Following Melanopsin Gene Therapy in the Degenerate Retina. Pupillometry and behavioral light avoidance indicated that subretinal OPN4 delivery restored or improved light responses; however, signaling to the visual cortex is not necessary to mediate such effects. To study cortical responses, we examined light-induced changes in visual cortex blood flow using laser speckle contrast imaging (Fig. 4*A*). Six months after subretinal delivery of OPN4, both eyes were stimulated by 480-nm light of 2-s duration and cerebral blood flow (CBF) recorded over the visual cortices. Treated mice showed an increase in CBF with an initial peak at 5.4 s after light onset, consistent with the peak expected in wild-type animals (25) (Fig. 4 *B* and *C* and Fig. S7*A*). There was no clear corresponding initial peak in the sham-injected group (Fig. S7*B*).

Finally, we assessed whether ectopic expression of OPN4 would aid image-forming vision. For this purpose, we used the one-trial spontaneous object recognition test (27, 28). In wild-type rodents with no retinal degeneration, a change in visual environment disrupts object recognition, indicating that these animals encode and remember the background visual environment in which an object is encountered (27, 28). By contrast, mice with visual deficits are not able to detect the visuospatial context of an object (29), indicating that they cannot encode visual information regarding their environment. Object recognition performance was analyzed to determine visual context recognition: this was determined by the ratio of time spent exploring a novel object relative to a previously encountered object. Two cohorts of mice were evaluated, one at 2 mo (Fig. S7*C*) and another at 13 mo after injection (Fig. 4*D*). Following OPN4 vector delivery 13 mo previously, treated mice showed a significant change in recognition ratio dependent on their visual environment ($P = 0.04$ for effect of visual context on object recognition performance; two-way ANOVA with Bonferroni

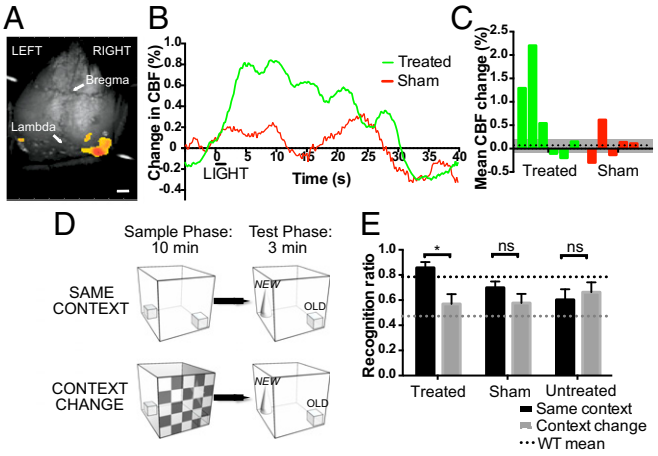

Fig. 4. Visual responses requiring image-forming vision are generated following melanopsin gene therapy in the degenerate retina. Laser speckle cortical imaging was used to measure changes in visual cortex blood flow following a 2-s, 480-nm light stimulus of 2,000-lx intensity (*A*). (Scale bar, 1 mm.) OPN4 vector-treated mice showed an appropriate light-dependent peak in cortical blood flow (CBF) compared with sham-injected controls (*B*; treated, $n = 5$; sham-injected, $n = 4$). The mean percentage change in CBF for each animal in the first 10 s after light onset is shown (*C*). The dashed line indicates mean change in sham-injected animals with SEM (gray). Visual context recognition testing (*D*): in the "same context" condition, the visual environment is identical in both phases. In the "Context Change" condition, there is a change in visual environment between phases, but all other factors are constant. The recognition ratio is calculated as $N/(N + f)$, that is, time spent exploring the novel object (N) as a fraction of the total time spent exploring both the novel and a familiar (f) object. Thirteen months after OPN4 vector delivery, recognition ratios for the novel object were significantly different in treated mice when the visual environment was the same versus when it was changed, indicating a visual environment-dependent change in behavior (*E*) ($P = 0.04$, two-way repeated-measures ANOVA with Bonferroni post hoc test; dashed line, wild-type mean, $^*P < 0.05$; treated, $n = 9$; sham-injected, $n = 8$; untreated, $n = 11$; ns, nonsignificant).

post hoc test; Fig. 4*E*). Combining younger and older cohorts, the effect of visual context on behavior was highly significant in the treated group overall ($P = 0.003$, split-plot ANOVA; Tables S1 and S2). No significant changes were seen in sham-injected or untreated control groups, suggesting an inability to form and retrieve an association between the object and visual context in these mice. Melanopsin vector-treated mice showed a behavioral pattern similar to that observed in wild-type mice with functional rods and cones in a test requiring image-forming vision.

Discussion

Data presented here demonstrate that a functional human melanopsin gene (OPN4) can be delivered to remaining retinal cells in a mouse model of end-stage retinal degeneration. This was achieved via subretinal injection of an AAV vector using a ubiquitous promoter, an approach currently validated in AAV gene therapy clinical trials (15, 16). Ectopically expressed OPN4 mediated depolarization of outer retinal cells and ultimately ganglion cell action potential firing, resulting in long-term restoration of the PLR and behavioral light avoidance up to at least 13 mo following injection. Finally, subretinal OPN4 expression led to light-induced changes in visual cortex blood flow and provided long-term improvements in a visually guided behavioral task that requires image-forming vision. In combination, these results suggest that this approach may be clinically useful in vision restoration in patients with end-stage RP.

In the interpretation of these data, a consideration is the mechanism by which visual responses were restored. We believe that responses detected arose from activation of retinal circuitry involved in image-forming vision rather than augmenting existing ipRGCs for several reasons. Human melanopsin was not detected by immunohistochemistry in ganglion cell membranes in transduced retinas. Similarly, light-induced c-Fos expression in vector-treated areas of retina was seen in multiple cells within the INL, whereas this pattern was not seen in the INL of controls. MEA recordings revealed a greater percentage of responsive electrodes in treated retinas compared with untreated controls, along with differences in firing rates and response kinetics, suggesting that a larger number of ganglion cells were generating light-induced action potentials in treated retinas.

To assess functional responses in vivo, a number of assessments were used including behavioral light avoidance since wild-type animals with functional rods and cones show aversion to bright light. Treated mice spent less time in the bright chamber compared with control mice, which showed an apparent preference for the bright chamber. This may be due to an inability of control mice to detect the difference in brightness between the two chambers resulting in exploration being guided primarily by nonvisual cues, for example, subtle differences in temperature, auditory, or olfactory cues. Interestingly, previous work including rodless/coneless mice has also demonstrated that mice have a preference for the front half of the chamber irrespective of whether the animal was placed there first or the test was performed in complete darkness (24).

Treated mice showed the ability to form and retrieve an association between an object and its visual environment in the visual context recognition task. In contrast, control groups were able to perform the object recognition task using nonvisual cues (since recognition ratios in these mice were above chance or 0.5), but performance did not vary according to visual environment. This test has been validated for the assessment of rod/cone-dependent image-forming visual responses (29). Previous work has also investigated the effect of changes in background irradiance on performance with wild-type mice requiring a substantial change in irradiance (e.g., an increase from 10 to 350 lx) to disrupt object recognition performance (29). Therefore, context-dependent behavior in treated mice is likely to be caused by the change in visual environment, rather than any changes in background irradiance caused by the different test arenas.

A potential concern is the effect of retinal remodeling seen in end-stage degeneration on restoration of visual function. Multiple changes within the remaining retina have been described in mouse models and human tissue (30–33), including neuronal morphological changes, cell death, network rewiring, and formation of gliosis between the retinal pigment epithelium and neural retina. Certain elements of remodeling such as the glial seal may potentially be overcome by subretinal injection, since the hydrostatic force generated could allow AAV to penetrate areas of gliosis. The process of remodeling does, however, demonstrate plasticity (30), and since we use a ubiquitous promoter to deliver melanopsin to the degenerate retina, it is possible that some of these abnormal connections from a variety of cells are used to restore visual responses. The clinical phenotype in human RP is of a rod–cone dystrophy in the majority of patients, which may also be variable with previous studies demonstrating differing degrees of degeneration even in the presence of the same genetic mutation and level of vision (34). Careful selection of potential patients for OPN4 optogenetic therapy would therefore be required since the ideal candidate would have severely affected vision yet grossly intact inner retinal structure (as visualized by ocular coherence tomography) and some remaining inner retinal function, detected for example using electrical phosphene testing (34, 35).

Human melanopsin as an optogenetic tool has significant advantages in its suitability for translation to patients. Being a native protein, OPN4 is unlikely to induce an immune response, and second, OPN4 shows greater light sensitivity than other optogenetic tools. We detected ganglion cell firing during MEA recordings at the lowest stimulus intensity tested (1.20×10^{12} photons·cm^{-2}·s^{-1}), whereas previous reports document a minimum stimulus of 1×10^{14} (36) or 1×10^{15}photons·cm^{-2}·s^{-1} (3) for

detection of ganglion cell responses following channelrhodopsin gene therapy and 1×10^{16} for halorhodopsin (4). We also report restoration of visually guided behavior in the visual context recognition task at a light intensity of 50 lx, corresponding to low-level indoor lighting. The brightest light stimulus we used was 2×10^{16} photons·cm^{-2}·s^{-1} during pupillometry (however, significant differences between groups were seen at lower intensities) or ≈13,000 lx (Table S3) equivalent to daylight conditions. The brighter stimulus intensity used for pupillometry in our experiments compared with previous studies using melanopsin likely reflects the use of different animal models (37) and our use of a 2-s white light stimulus (chosen to be a more useful stimulus for image-forming vision), whereas other studies used monochromatic light (37) and longer stimulus durations more suited for activating ipRGCs (5).

The quality of vision that might be restored by OPN4 gene therapy is likely to be affected by its response kinetics. Although slower than classical (rod/cone) photopigments, the detection of transient light responses following melanopsin stimulation (Fig. S4*B*) as previously described (38) may be a useful input for image-forming vision. Furthermore, not all ganglion cell spikes are transmitted at the retinogeniculate synapse allowing for modification of the visual signal (39). Melanopsin gene therapy may provide functionally useful vision in a static visual environment such as in the visual context recognition test, which may be useful to patients in terms of aiding navigation. For more dynamic environments, modification of the visual input through devices such as image-processing glasses (40) may be required.

The use of human melanopsin delivered via subretinal injection using a CBA promoter for optogenetic restoration of vision has not previously been described. We demonstrate effective transduction of end-stage degenerate retina resulting in sustained restoration of visual function. The effects may be mediated by transduction of bipolar and horizontal cells. This approach has significant potential for translation to patients since, although technically more challenging, subretinal delivery has been established as safe in current clinical trials and provides the advantage of delivering a high concentration of vector to residual retinal cells, whereas the alternative method of intravitreal delivery may not be as effective in humans. Targeting the outermost surviving retinal layers will likely allow greater levels of signal processing to be performed by existing retinal circuitry, potentially resulting in restoration of more complex visual responses.

Materials and Methods

All animal experiments were conducted as part of a programme of work assessed by the Clinical Medicine Animal Welfare and Ethics Review board of the University of Oxford and legally approved by the U.K. Home Office. They were also conducted in accordance with Association for Research in Vision and Ophthalmology statements on care and use of animals in ophthalmic research. C3H/HeNHsd-*Pde6b*^{rd1} (*rd1*) mice were 6–8 wk old at time of intraocular injection. Treated eyes were injected with a dose of 1.5×10^9 viral genomes (vg) per eye of AAV2/8(Y733F) CBA-*OPN4*-IRES-DsRed vector, with an equivalent volume of PBS injected in sham-treated eyes and age-matched untreated eyes also used as controls. Further experimental details are described in *SI Materials and Methods*, Tables S4 and S5.

ACKNOWLEDGMENTS. Funding was provided by Wellcome Trust, National Institute for Health Research Biomedical Research Centres of Oxford and Moorfields, Medical Research Council, Biotechnology and Biological Sciences Research Council, and Royal College of Surgeons of Edinburgh.

1. Bessant DA, Ali RR, Bhattacharya SS (2001) Molecular genetics and prospects for therapy of the inherited retinal dystrophies. *Curr Opin Genet Dev* 11:307–316.
2. Stingl K, et al. (2013) Artificial vision with wirelessly powered subretinal electronic implant alpha-IMS. *Proc Biol Sci* 280:20130077.
3. Lagali PS, et al. (2008) Light-activated channels targeted to ON bipolar cells restore visual function in retinal degeneration. *Nat Neurosci* 11:667–675.
4. Busskamp V, et al. (2010) Genetic reactivation of cone photoreceptors restores visual responses in retinitis pigmentosa. *Science* 329:413–417.
5. Lin B, Koizumi A, Tanaka N, Panda S, Masland RH (2008) Restoration of visual function in retinal degeneration mice by ectopic expression of melanopsin. *Proc Natl Acad Sci USA* 105:16009–16014.
6. Cehajic-Kapetanovic J, et al. (2015) Restoration of vision with ectopic expression of human rod opsin. *Curr Biol* 25:2111–2122.
7. Bi A, et al. (2006) Ectopic expression of a microbial-type rhodopsin restores visual responses in mice with photoreceptor degeneration. *Neuron* 50:23–33.
8. Provencio I, Jiang G, De Grip WJ, Hayes WP, Rollag MD (1998) Melanopsin: An opsin in melanophores, brain, and eye. *Proc Natl Acad Sci USA* 95:340–345.
9. Provencio I, et al. (2000) A novel human opsin in the inner retina. *J Neurosci* 20:600–605.
10. Doroudchi MM, et al. (2011) Virally delivered channelrhodopsin-2 safely and effectively restores visual function in multiple mouse models of blindness. *Mol Ther* 19:1220–1229.
11. Cronin T, et al. (2014) Efficient transduction and optogenetic stimulation of retinal bipolar cells by a synthetic adeno-associated virus capsid and promoter. *EMBO Mol Med* 6:1175–1190.
12. Hughes S, et al. (2015) Using siRNA to define functional interactions between melanopsin and multiple G protein partners. *Cell Mol Life Sci* 72:165–179.
13. Panda S, et al. (2005) Illumination of the melanopsin signaling pathway. *Science* 307:600–604.
14. Melyan Z, Tarttelin EE, Bellingham J, Lucas RJ, Hankins MW (2005) Addition of human melanopsin renders mammalian cells photoresponsive. *Nature* 433:741–745.
15. Cideciyan AV, et al. (2008) Human gene therapy for RPE65 isomerase deficiency activates the retinoid cycle of vision but with slow rod kinetics. *Proc Natl Acad Sci USA* 105:15112–15117.
16. MacLaren RE, et al. (2014) Retinal gene therapy in patients with choroideremia: Initial findings from a phase 1/2 clinical trial. *Lancet* 383:1129–1137.
17. van Wyk M, Pielecka-Fortuna J, Löwel S, Kleinlogel S (2015) Restoring the ON switch in blind retinas: Opto-mGluR6, a next-generation, cell-tailored optogenetic tool. *PLoS Biol* 13:e1002143.
18. Dalkara D, et al. (2013) In vivo-directed evolution of a new adeno-associated virus for therapeutic outer retinal gene delivery from the vitreous. *Sci Transl Med* 5:189ra76.
19. Dalkara D, et al. (2009) Inner limiting membrane barriers to AAV-mediated retinal transduction from the vitreous. *Mol Ther* 17:2096–2102.
20. Kotterman MA, et al. (2015) Antibody neutralization poses a barrier to intravitreal adeno-associated viral vector gene delivery to non-human primates. *Gene Ther* 22:116–126.
21. Carter-Dawson LD, LaVail MM, Sidman RL (1978) Differential effect of the rd mutation on rods and cones in the mouse retina. *Invest Ophthalmol Vis Sci* 17:489–498.
22. Sheng M, McFadden G, Greenberg ME (1990) Membrane depolarization and calcium induce c-*fos* transcription via phosphorylation of transcription factor CREB. *Neuron* 4:571–582.
23. Semo M, Lupi D, Peirson SN, Butler JN, Foster RG (2003) Light-induced c-*fos* in melanopsin retinal ganglion cells of young and aged rodless/coneless (*rd/rd cl*) mice. *Eur J Neurosci* 18:3007–3017.
24. Semo M, et al. (2010) Dissecting a role for melanopsin in behavioural light aversion reveals a response independent of conventional photoreception. *PLoS One* 5:e15009.
25. Singh MS, et al. (2013) Reversal of end-stage retinal degeneration and restoration of visual function by photoreceptor transplantation. *Proc Natl Acad Sci USA* 110:1101–1106.
26. Ray TA, et al. (2014) GPR179 is required for high sensitivity of the mGluR6 signaling cascade in depolarizing bipolar cells. *J Neurosci* 34:6334–6343.
27. Mumby DG, Gaskin S, Glenn MJ, Schramek TE, Lehmann H (2002) Hippocampal damage and exploratory preferences in rats: Memory for objects, places, and contexts. *Learn Mem* 9:49–57.
28. Dix SL, Aggleton JP (1999) Extending the spontaneous preference test of recognition: Evidence of object-location and object-context recognition. *Behav Brain Res* 99:191–200.
29. Tam SK, et al. (2016) Modulation of recognition memory performance by light requires both melanopsin and classical photoreceptors. *Proc Biol Sci* 283:20162275.
30. Jones BW, et al. (2003) Retinal remodeling triggered by photoreceptor degenerations. *J Comp Neurol* 464:1–16.
31. Marc RE, Jones BW (2003) Retinal remodeling in inherited photoreceptor degenerations. *Mol Neurobiol* 28:139–147.
32. Jones BW, et al. (2016) Retinal remodeling in human retinitis pigmentosa. *Exp Eye Res* 150:149–165.
33. Milam AH, Li ZY, Fariss RN (1998) Histopathology of the human retina in retinitis pigmentosa. *Prog Retin Eye Res* 17:175–205.
34. Jacobson SG, Sumaroka A, Luo X, Cideciyan AV (2013) Retinal optogenetic therapies: Clinical criteria for candidacy. *Clin Genet* 84:175–182.
35. Naycheva L, et al. (2012) Phosphene thresholds elicited by transcorneal electrical stimulation in healthy subjects and patients with retinal diseases. *Invest Ophthalmol Vis Sci* 53:7440–7448.
36. Macé E, et al. (2015) Targeting channelrhodopsin-2 to ON-bipolar cells with vitreally administered AAV restores ON and OFF visual responses in blind mice. *Mol Ther* 23:7–16.
37. Lucas RJ, Douglas RH, Foster RG (2001) Characterization of an ocular photopigment capable of driving pupillary constriction in mice. *Nat Neurosci* 4:621–626.
38. Sekaran S, Foster RG, Lucas RJ, Hankins MW (2003) Calcium imaging reveals a network of intrinsically light-sensitive inner-retinal neurons. *Curr Biol* 13:1290–1298.
39. Guido W, Lu SM (1995) Cellular bases for the control of retinogeniculate signal transmission. *Int J Neurosci* 80:41–63.
40. Hicks SL, et al. (2013) A depth-based head-mounted visual display to aid navigation in partially sighted individuals. *PLoS One* 8:e67695.
41. LaVail MM, Matthes MT, Yasumura D, Steinberg RH (1997) Variability in rate of cone degeneration in the retinal degeneration (*rd/rd*) mouse. *Exp Eye Res* 65:45–50.
42. Koistinaho J, Sagar SM (1995) Light-induced c-*fos* expression in amacrine cells in the rabbit retina. *Brain Res Mol Brain Res* 29:53–63.
43. Hughes S, et al. (2016) Characterisation of light responses in the retina of mice lacking principle components of rod, cone and melanopsin phototransduction signalling pathways. *Sci Rep* 6:28086.
44. Lucas RJ, et al. (2014) Measuring and using light in the melanopsin age. *Trends Neurosci* 37:1–9.